Journal of
Marine Science and Engineering

MDPI

Article

Field Investigation on the Coastal Erosion and Progradation Evolution of the Binzhou Shelly Chenier in China: Comparisons between Normal and Typhoon Hydrodynamics

Mingzheng Wen [1,2,3], Huaibo Zhang [4], Shoujun Wang [4], Zhiwen Shang [1,2,3], Shaotong Zhang [5], Peng Yang [1,2,3] and Hong Wang [1,2,3,*]

1 Tianjin Centre, China Geological Survey, Tianjin 300170, China; wenmzh@foxmail.com (M.W.); shangzhiwen1007@126.com (Z.S.); dcyangpeng@163.com (P.Y.)
2 CGS Key Laboratory of Coast Geo-Environment, Tianjin 300170, China
3 North China Center of Geoscience Innovation, Tianjin 300170, China
4 Binzhou Shell Dike Islands and Wetlands National Nature Reserve, Binzhou 251900, China; sdwdzhb@163.com (H.Z.); sdwdwsj@163.com (S.W.)
5 Key Laboratory for Submarine Geosciences and Prospecting Techniques (Ministry of Education), College of Marine Geosciences, Ocean University of China, Qingdao 266100, China; shaotong@ouc.edu.cn
* Correspondence: whong@163.com

Abstract: The shelly chenier is a dike-like accumulation formed by waves, currents, and other hydrodynamic forces pushing the shells and their debris in the intertidal zone to the high tide line. It is a special type of coastal dike. The shelly chenier located in Wangzi Island of northern Shandong Province is the last well-preserved chenier of the Bohai Bay with natural attributes exposed on the surface. It has unique and irreplaceable attributes among the shell beaches of China. Based on remote sensing interpretation, field investigation, and GPS-RTK (Real-Time Kinematic) measurement, this paper investigates the coastal erosion and progradation evolution of the Binzhou Shelly Chenier in China usingcomparisons between normal and typhoon hydrodynamics. The results show that: (1) There are two kinds of shelly chenier in the study area, the first is "the tidal channel shelly chenier" which is significantly affected by the tidal current, and the second is "the open shelly chenier", which is significantly affected by direct scouring and silting of waves. The open shelly chenier is continuously eroding under the normal hydrodynamics and the shell beach is supplied by a large number of shells and their debris under the typhoon hydrodynamics, while the tidal channel shelly chenier is gradually developed due to the action of alongshore currents and in–out flows. (2) The energy of waves and currents under normal hydrodynamics is insufficient to transport the shells and their debris in the intertidal zone to the shell-beach. On the contrary, the continuous action of waves makes the shells and their debris on the open-shell beach finer and transports the shells and their debris to the sea causing erosion and retreat of the shelly chenier. (3) The action of typhoons and other strong winds and waves results in the original accumulation on the open shell-beach being further transported to the land and provides a large amount of shells and debris from the intertidal zone to the shelly chenier. Based on GPS-RTK monitoring data from 2020–2021, it was found that the transport volume of shells and debris caused by a typhoon storm surge is equivalent to the annual transport volume under normal ocean dynamics.

Keywords: typhoon storm surge; normal hydrodynamics; erosion and deposition; remote sensing; field survey

check for updates

Citation: Wen, M.; Zhang, H.; Wang, S.; Shang, Z.; Zhang, S.; Yang, P.; Wang, H. Field Investigation on the Coastal Erosion and Progradation Evolution of the Binzhou Shelly Chenier in China: Comparisons between Normal and Typhoon Hydrodynamics. *J. Mar. Sci. Eng.* **2022**, *10*, 752. https://doi.org/10.3390/jmse10060752

Academic Editor: Anabela Oliveira

Received: 9 April 2022
Accepted: 26 May 2022
Published: 30 May 2022

Publisher's Note: MDPI stays neutral with regard to jurisdictional claims in published maps and institutional affiliations.

Copyright: © 2022 by the authors. Licensee MDPI, Basel, Switzerland. This article is an open access article distributed under the terms and conditions of the Creative Commons Attribution (CC BY) license (https://creativecommons.org/licenses/by/4.0/).

1. Introduction

The word chenier derives from the Cajun name for oak, chêne, which is the prevalent tree encroaching sand ridges in southwestern Louisiana [1]. In geomorphology, the term "chenier" designates a body of wave-reworked coarse-grained sediment resting stratigraphically on a muddy substrate [2,3]. Unlike beach ridges, cheniers are not common because

their genesis depends on a specific balance between sediment availability and wave action; thus, they will only develop where cohesive sediments are available in large volumes with enough sand, shelly deposits, or gravel that can be reworked by waves [4–6]. Cheniers are widely distributed on the coastal plains of the world, of which the northernmost is located on the coastal areas of the former Soviet Union in the north, and the southernmost is located on the coasts of northern Australia and New Zealand in the south [7]. Cheniers are also located in Bohai Bay, Northern Jiangsu, and the Yangtze River Delta in China [8–11].

The three most ancient chenier plains of the world arein southwestern Louisiana in the USA, Suriname, and the Yellow River Delta of China [12–15]. Draut et al. indicate that cheniers in Louisiana might have formed during strong storms in the presence of fluid muds and energetic wave climates [13]. Anthony et al. investigated the formation of one of the largest chenier plains systems on Earth along the Guyanese coast of South America [14]. These cheniers develop as a result of the migration of mud banks from the mouths of the Amazon and Orinoco River deltas [14,15]. With prominent characteristics such as a long history (~7000 years) and wide distribution (~43,500 ha), the chenier plain in the Yellow River Delta is considered as a natural laboratory for Quaternary geological research [16–24]. In the early 1960s, Li and Wang carried out the first study of cheniers in China and used the chenier as evidence for the existence of ancient shorelines [10,23]. Wang Hong put forward the multi-cause theory of the chenier which is located in the Yellow River Delta of China. He believed that the chenier is the transition between the barrier island and the coastal dike [24]. Cheniers, which are located on the west and southwest coast of Bohai Bay, are also called shell-cheniers because they are mainly composed of shells and their debris [10,23]. The formation of the shelly chenier is closely related to the migration of the Yellow River (Figure 1A). From Ad 11 to 1128, the Yellow River migrated several times, forming a large-scale and shallow silty muddy coast in the study area, which laid the foundation for the development of shelly cheniers in this area. From 1128 to 1855, the Yellow River diverted south into the Yellow Sea. The coast from the Dakou River estuary to the Majia estuary was in a stable state for a long time, and the shelly chenier continued to grow. From 1904 to 1976, the Yellow River entered the sea to the east of the Majia River estuary, and the land silted into the sea, resulting in the formation of a wide V-shaped coast from Tianjin Qikou to the middle of the modern Yellow River Delta (Figure 1B). The huge changes in the coastline's outline within a short time (about 70 years) changed the local tidal environment, resulting in intensified erosion. The lateral transport of sediment from the Yellow River into the sea to Wangzi Island could have caused the progradation of the coast or guaranteed stability, but this was offset by the enhanced tidal erosion. Under the combined action of wave and tidal currents, the coast was eroded, and shelly cheniers were cut up into several remaining alluvial islands [25].

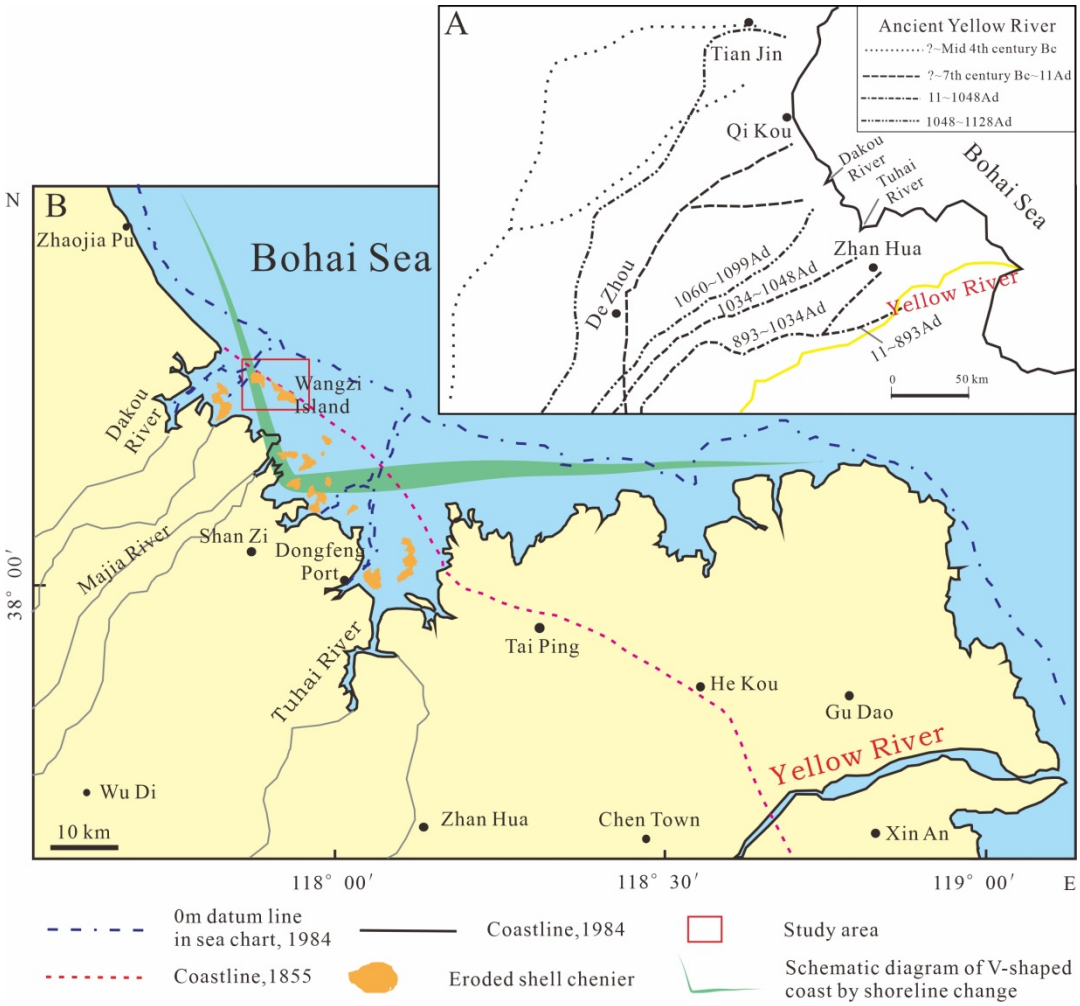


Figure 1. (**A**): Location of the Yellow River mouth before 1128; (**B**): The coastlines from the Dakou River mouth to the Tuhai River mouth in 1855 and 1984 (According to references [25–27]).

Under the dual influence of natural factors such as storm surges and coastal erosion and human activities such as coastal engineering, most of the shelly cheniers distributed along the modern coastline have disappeared. At present, only the shelly cheniers located in Shanggulin in Dagang, Tianjin, the Houtang Pu in Huanghua, Hebei and Wngzi Island, Wudi, Shandong have been protected, but most of them have lost their natural attributes. The shelly chenier located in Wangzi Island of northern Shandong Province is the last well-preserved chenier of the Bohai Bay with natural attributes exposed on the surface. It has unique and irreplaceable attributes among the shell–beaches of China. The decrease of sediment supply affects the reproduction of shellfish, and the two ports (Huanghua port and Binzhou port) change the offshore marine dynamic conditions, which leads to a lack of adequate supply of shell and their debris on the shell–beach. In addition, many factors such as salt field construction, shell mining, and excavation of aquaculture ponds have gradually eroded the shelly chenier in the study area [28–30]. Previous studies have shown that there were 12 shelly chenier islands in this area in 1956, with a total area of about 11.24 km^2. By 2005, there were only 6 shelly chenier islands with an area of only 2.59 km^2 [31]. In addition, extreme hydrodynamics such as typhoon storm surges further exacerbated the damage of the shelly chenier Island: Typhoon Lekima in 2019 made the shell–beach move landward, and the mud layer originally buried under the shell beach was generally exposed [32]. Based on remote sensing interpretation, field investigation, and GPS-RTK (Real-Time Kinematic) measurement, this paper investigates the coastal erosion and progradation evolution of the Binzhou Shelly Chenier in China, using comparisons

between normal and typhoon hydrodynamics. Our investigation and research can help us understand the erosion process of the shelly chenier and can inform shelly chenier conservation and restoration efforts.

2. Study Area

The study site (117°55′ E, 38°14′) is located in the Binzhou Shell Dike Islands and Wetlands National Nature Reserve, the core area of chenier plain ecosystems in the Yellow River Delta, China (Figure 2A,B). The shelly chenier is distributed near the high tide line from the Dakou River Estuary to the Majia River estuary, which runs parallel to the coastline and is distributed in a NW–SE direction. The chenier is tens to hundreds of meters wide and 1–3 m thick [19]. Since the 1980s, due to the interference of embankment construction, aquaculture, salt fields, oil production, and port construction, the coastline in this area has rapidly advanced seaward and shortened, and the natural coastline has been gradually replaced by the artificial coastline. The breakwater of the Huanghua Port Coal Terminal, which is about 20 km long in the northwest, and the west breakwater of Binzhou Port, which is about 15 km long in the southeast, together with the shelly chenier, form a U-shaped artificial bay. The shell coast between the Dakou River and the Majia River is located at the top of the U-shaped artificial bay; the shelly chenier is in an environment surrounded by artificial coastlines [33].

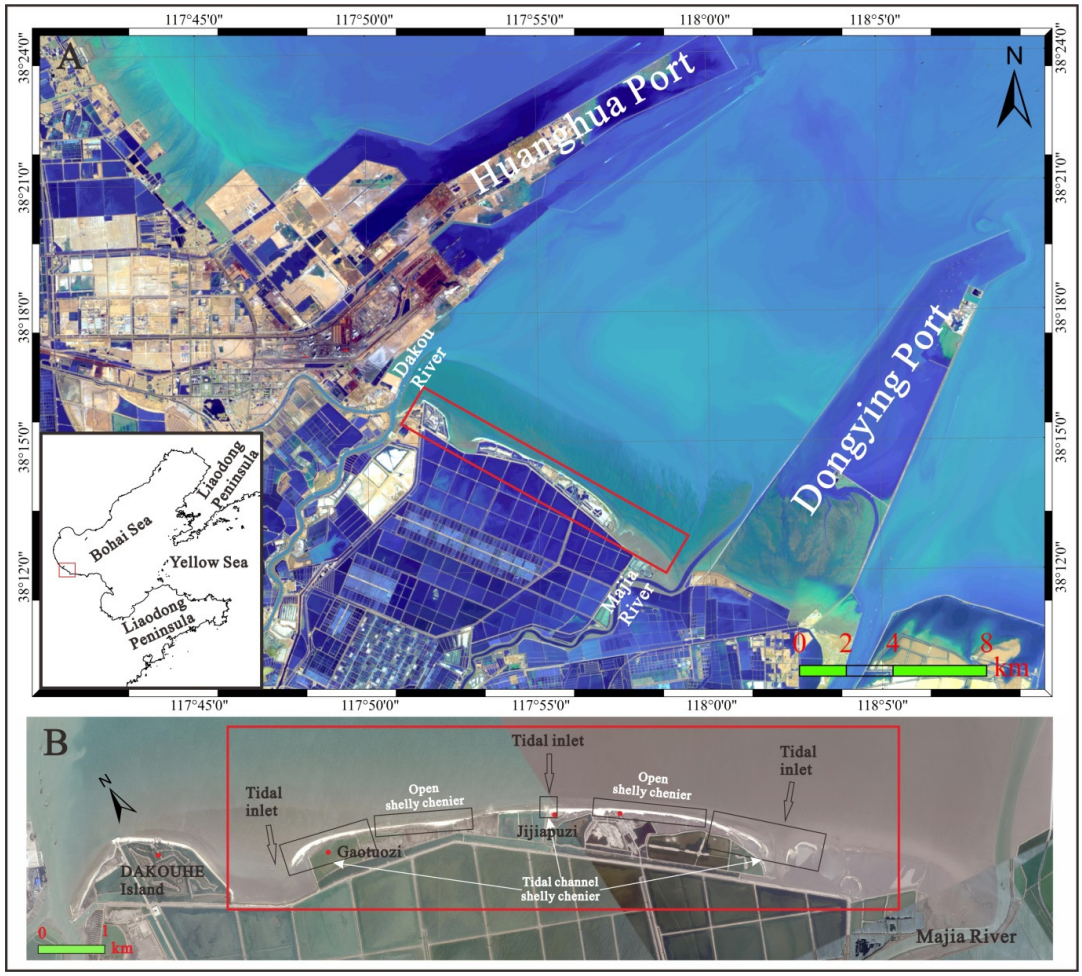


Figure 2. **(A)** The geographical location of the study area, (**B**) The classification of shelly cheniers, Tidal channel shelly chenier: located near the tidal inlet and significantly affected by tidal current; Open shelly chenier: significantly affected by direct scouring and silting of waves.

The tidal characteristic in the study is irregular semidiurnal tide, with an average tidal range of 221 cm and a maximum tidal range of 355 cm. The maximum tidal current in the coastal waters is 80–114 cm/s. The current velocity outside of the Dakou River estuary is the largest. The maximum monthly average wave height is 0.7 m, which was recorded appeared in May and November, and the minimum value was 0.5 m, which appeared in July and August. The main waves are directed to NEE–E and NE–SEE, with frequencies of 20% and 38%, respectively. Strong waves are directed to ENE–E, with a maximum wave height of 3.0–3.3 m. Storm surge frequently happened in the area. From 1945 to 1985, 117 storm surges with an increase of more than 1 m occurred, on an average of 3 to 4 times per year. Since the 1960s, there have been three major storm surges, with a maximum water increase of about 300 cm. The shelly cheniers in the study area can be grouped into two categories: tidal channel shelly chenier and open shelly cheniers according to their environment [31]. The former are located near the tidal inlet and is significantly affected by the tide, while the latter are significantly affected by direct scouring and silting of waves, as shown in Figure 2.

3. Research Methods

In this paper, the coastal erosion and progradation evolution of the Binzhou Shelly Chenier are investigated and studied through remote sensing interpretation, on-site typical landform investigation, and GPS-RTK elevation measurement. The layout of the survey points is shown in Figure 3. Satellite remote sensing data has the characteristics of strong periodicity, intuitive images, obtaining instantaneous ground information, large coverage area, and good synchronization effect. In this paper, using Locaspaceviewer (LSV) 3D Digital Earth software, the multiphase remote sensing images of tidal channel shelly cheniers A1, A3, and open shell chenier A2 in the study area from 2003 to 2017 are selected as the data source. A1 is located near Gaotuozi, covering an area of about 0.70 km^2, with a total of 6 remote sensing images; A3 is located in the northwest of the Majia River estuary, covering an area of about 0.98 km^2, with three remote sensing images; A2 is located near the trestle of Wangzi Island, with an area of about 0.19 km^2, with four remote sensing images, as shown in Figure 3A. The shelly chenier of Binzhou is mainly composed of shells, shell fragments, shell debris, and medium and fine sand. The content of shells and debris is as high as 70~95%. In the remote sensing image, the shelly chenier island is bright white, and the edge line of the shelly chenier island is easy to distinguish. This paper uses the visual interpretation method to extract the boundary range of the shelly chenier island and verifies it in combination with the field investigation.

We carried out a periodic geomorphic survey on the typical geomorphic survey points, and recorded the changes in the beach surface of the shelly chenier through the on-site camera. We selected 3 typical survey points: P1 is located in the tidal channel shelly chenier, and P2 and P3 are located in the open shelly chenier, with P2 located in A2. To better compare and analyze the erosion and progradation process of the shelly chenier, the beach profile elevation of the shelly chenier in the study area was measured in July 2020, September 2020, and January 2021 respectively. The iRTK5x high-precision inertial navigation measurement system was adopted, the positioning accuracy of the system was 3 cm, and the RTK Positioning accuracy was the plane: $\pm(8 + 1) \times 10^{-6}$ D) mm; Elevation: $\pm(15 + 1) \times 10^{-6}$ D) mm; Static positioning accuracy: plane: $\pm(2.5 + 0.5) \times 10^{-6}$ D) mm; Elevation: $\pm(5 + 0.5) \times 10^{-6}$ D) mm (D is the distance between measured points). Five GPS-RTK elevation survey profiles (L1–L5) were set in the study area to monitor the erosion and deposition process of the shelly chenier. L1–L3 wass located on the tidal channel shelly chenier near the tidal inlet of Jijiapuzi; L1 was perpendicular to the tidal inlet and L2–L3 was perpendicular to the coastline. L4–L5 was located on the open shelly chenier, while L4 was located at A2 of the Wangzi Island trestle, and perpendicular to the coastline; L5 was located at the Arsenal Memorial Pavilion of the Hebei-Shandong border military region, perpendicular to the coastline.

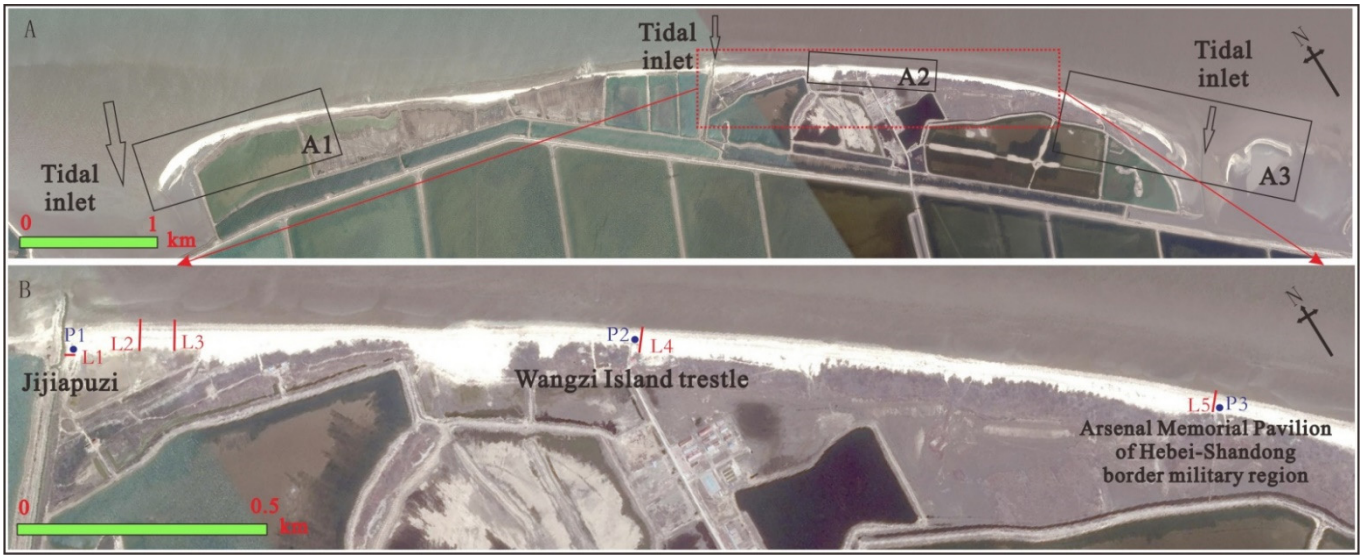


Figure 3. (**A**): Location of remote sensing interpretation areas A1–A3. (**B**): Layout of field investigation, L1–L5 are the GPS-RTK elevation survey profiles, and P1–P3 are the geomorphic survey points. A1, A3, L1–L3, and P1 are located in the tidal channel shelly chenier, and A2, L4–L5, and P2–P3 are located in the open shelly chenier.

4. Results

4.1. Remote Sensing Interpretation

The left side of Figure 4 shows the remote sensing images of the A1–A3 areas in the past 20 years, and on the right is the change in seashell beach edge recognized by the remote sensing image. From 2003 to 2005, the shelly chenier in A1 was developed close to the dike of the artificial fishpond. From 2008 to 2017, it gradually extended to the vast tidal flat in the northwest, forming a shell cape in the northwest corner. In area A1, the right side of the beach surface edge line of the shelly chenier, which is parallel to the coastline area, was eroding year by year. The shelly chenier on the corner of the left of the area A1 is rapidly expanding to the sea. The beach width and range of the shelly chenier in area A2 decreased in 2011 compared with 2008. In 2013 and 2017, the shelly chenier in area A2 expanded significantly to the land compared with 2011. From 2011 to 2017, the beach surface edge line of the shelly chenier gradually eroded landward. In 2011, the development scope of the shelly chenier in area A3 was small and discontinuous. From 2013 to 2017, the shelly chenier on the left side of area A3 was developed and tended to be integrated. A new tidal inlet channel was gradually formed in the middle of area A3, and a new crescent-shaped shelly chenier was gradually formed on the right side of the tidal inlet channel from 2011 to 2017, while the sea-side line of the shelly chenier was gradually pushed inland. The newly formed crescent-shaped shelly chenier gradually extended to both sides. The comparative analysis of remote sensing images shows that the edge line of the open shelly chenier in the study area retreats year by year. The tidal channel shelly cheniers in areas A1 and A3, are forming a new shelly chenier cape in the northwest corner and a new crescent-shaped shell-beach in the southeast direction.

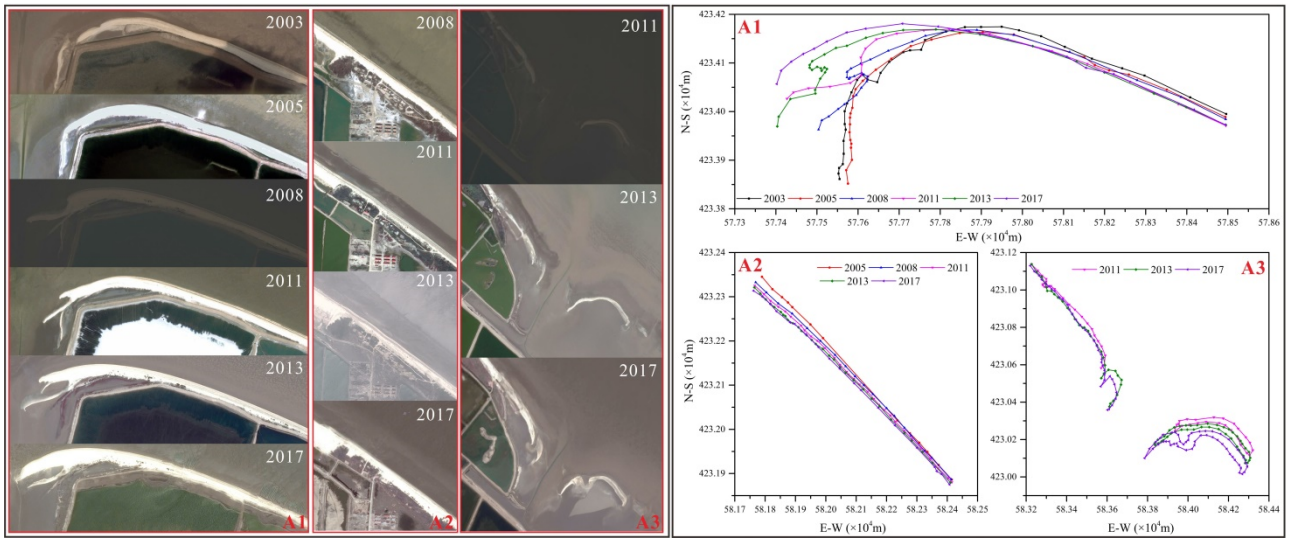


Figure 4. Left: Remote sensing images of the shelly chenier, **right**: change in the seashell beach edge recognized from a remote sensing image; A1 and A3 are tidal channel shelly cheniers and A2 is an open shelly chenier.

4.2. Typical Geomorphic Survey

The geomorphic changes are shown in Figure 5. Figure 5A shows the geomorphic change at point P1, which is located near the Jijiabaozi tidal inlet. The typhoon Lekima on 10–12 August 2019 caused the erosion of 2–3 m thick artificial argillaceous accumulation on both sides of the artificial tidal inlet of the original aquaculture pond, exposing the underlying mud layer. At the same time, the artificial tidal inlet was significantly widened and deepened under the action of typhoon Lekima, forming a tidal channel with a width of about 10 m and a water depth of >1 m. According to the survey on 29 October 2019, several sand dams with an area of hundreds of thousands of square meters and 10–20 cm higher than the normal beach surface were formed on the high marsh, and the surface of sand dams was covered with a large number of shells and debris.

Figure 5B shows the geomorphic change of point P2, which is located near the trestle of Wangzi island. It belongs to an open shelly chenier. Before the typhoon Lekima (before 11 August 2019), shells and their debris accumulated more than 1m high in front of the trestle. After Typhoon Lekima (13 August 2019), the shells and their debris with 1 m thickness were all transported elsewhere. After that, the beach surface of the shelly chenier was continuously eroded to the land, and the shells and their debris on the shell-beach surface were gradually refined under the long-term action of waves and tidal currents. The investigation results on 1 July 2020 showed that all the "columns" on the trestle table were damaged, the right side of the trestle table was significantly tilted due to erosion, and the three large stone slabs on the shell-beach surface were "missing". An image from January 2021 shows that the shell-beach width is further shortened, and there is only a thin layer of shell and debris accumulation in the upper layer, while the "mud layer" of the lower layer can be seen.

Point P3 at the Arsenal Memorial Pavilion of the Hebei Shandong border military region is shown in Figure 5C. After Typhoon Lekima, three shell accumulations parallel to the coastline were formed on the shell-beach surface, which are composed of single-lobe (partial double-lobe) shells, and the supplied shells were gradually evenly distributed on the shell-beach under the action of later waves and currents. A *Tamarix* in the red frame of Figure 5C, the distance between the *Tamarix* and the junction of the shell–beach and the muddy tidal is gradually shortened, indicating that the shell-beach surface is gradually eroding to the land under the action of marine dynamics (July 2019–January 2021). Figure 5D shows the shells and debris accumulated by Typhoon Lekima with a

height of ~50 cm, and the tidal channel shelly chenier continuously developed under the action of the tide, respectively.



Figure 5. Typical geomorphic changes under the action of normal and typhoon hydrodynamics (Typhoon Lekima: 10–12 August 2019), (**A**): P1, belonging to the tidal channel shelly chenier; (**B**) is point P2 and (**C**) is point P3, which belong to the open shelly chenier; (**D**): Changes in the shelly chenier under the action of Typhoon Lekima and the tidal current.

4.3. Beach Profile Elevation Survey

The results of the elevation survey with GPS-RTK in the beach profile of the shelly chenier are shown in Figure 6. The lines L1–L3 are located on the tidal channel shelly chenier of the Jijiapuzi tidal inlet. In July 2019, the tidal channel was relatively narrow and shallow. After typhoon Lekima, the depth and width of tidal channels have been greatly expanded. L1 started from the residual argillaceous accumulation on the southeast side of the tidal channel. In July 2020, the argillaceous accumulation was about 0.3 m higher than the shell-beach surface. The residual argillaceous accumulation was completely eroded in July and August 2021. The tidal channel extended about 6 m to both sides, and the maximum erosion thickness of the shell-beach was about 1.5 m.

There are three periods of monitoring data in line L2, which are January 2021, July 2021, and August 2021, respectively. From January to July 2021, a large number of shells and their debris was transported to the shell-beach, with a handling volume of about 3.14 m^3 per unit length. From July to August 2021, affected by Typhoon In-fa (25–30 July 2021), the shells and their debris originally transported to the beach were further transported to the shore and piled up on the upper part of the shell-beach to form aeolian dunes, with a length of about 7.03 m^3 per unit length. The results of L3 show that a large number of shells and their debris were transported from the foot of the shell-beach to the upper from

July 2020 to July 2021. After Typhoon In-fa, the shells and their debris on the shell-beach were further transported to the landside.

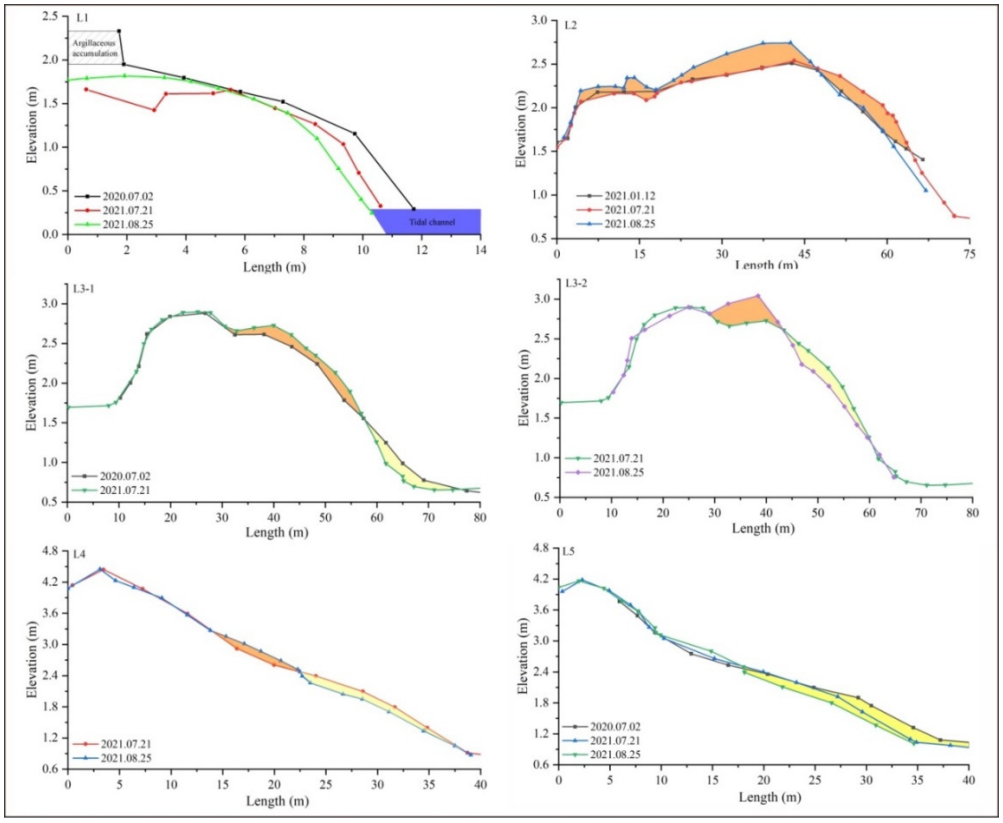


Figure 6. The results of the beach profile elevation survey with GPS-RTK. Line L1–L3 belongs to the tidal channel shelly chenier; line L4–L5 belongs to open shelly chenier. The colored fill between lines indicates the amount of erosion or accretion, where yellow stands for erosion, while orange stands for accretion. Typhoon In-fa occurred on 22–25 July 2021.

L4 is located near the trestle of Wangzi island and belongs to an open shelly chenier. The monitoring results show that the shell-beach in this area is gradually being eroded. During the period from July to August 2021, the net erosion of the shell-beach caused by the Typhoon In-fa was about 1.03 m^3, of which the erosion of the shell and its debris per unit length was about 1.96 m^3 (lower part of the shell-beach) and the accumulation is about 0.93 m^3 per unit length (middle of the shell-beach). L5 is located in the front of the Arsenal Memorial Pavilion of the Hebei Shandong military region, where the shell beach has been eroded. From July 2020 to July 2021, the unit length erosion of the shell and its debris under the action of normal marine dynamics was about 2.49 m^3, and under the action of Typhoon In-fa from July 2012 to August 2021, it was about 2.20 m^3.

5. Analysis

The results of the remote sensing interpretation, geomorphic survey, and elevation monitoring show that the open shelly chenier is in the process of erosion and regression (Figure 4: A2, and geomorphic survey points B and C in Figure 5); the *Tamarix* in Figure 5C, as a marker point, more clearly shows the process of erosion and regression of the shell-beach. On the other hand, the GPS-RTK elevation measurement results of survey lines L4–L5 also show the erosion and regression process of the shelly chenier. Generally, the velocity of the rising tide is greater than that of the falling tide in the intertidal zone, which is conducive to the shore transportation of shells and their debris [34]. However, the intensity of the current power and wave height will be reduced moderately due to the

sheltering effect of the long breakwaters of Huanghua Port and Binzhou Port. The shelly chenier beach cannot be effectively supplied with shells and their debris under the normal hydrodynamics. At the same time, fine-grained shell debris is constantly transported to the sea, resulting in shelly chenier erosion. For the tidal channel shelly chenier, the seawater enters the tidal channel, and the flow velocity decreases during flood tide. And at ebb tide, the sea water converges, and the ebb tide velocity increases gradually. The tidal channel is widened under the action of tidal erosion, and as shown in the beach profile L1 in Figure 6, the tidal channel extended about 6m to both sides. The remote sensing interpretation results of A1 and A3 in Figure 4 show the expansion process of the shelly chenier. Beach A1 gradually extended to the vast tidal flat in the northwest, forming a shell cape in the northwest corner. However, the right side running parallel to the coastline area of A1 beach was eroding year by year. Therefore, the progradation of the tidal channel shelly chenier may be attributed to the erosion and transportation of the right beach under the action of alongshore current and in–out flow.

Compared with normal hydrodynamics, typhoon storm surges cause stronger waves and currents, which are generally considered to be the main dynamic factor for the formation of shelly cheniers [13,35]. Typhoon Lekima turned westward after entering the Shandong Peninsula and lingered for a long time, causing sustained northeast wind stronger than force 8 [36]. While the storm surge caused damage to the shelly chenier in this area, it also provided a large amount of shell and debris supply for the shelly chenier (Figure 5). At the geomorphic survey point P1, under the action of Typhoon Lekima, a shell-sand dam with a total area of about 5000 m^2 was formed in the upper part of the intertidal zone, which is covered by a large amount of shells and debris. The elevation comparison of survey line L4 before and after the storm surge shows that during Typhoon In-fa in 2021, part of the shells and their debris on the shell beach accumulated to the land side and the other part was transported to the sea, resulting in an average thickness reduction of about 20 cm within 17 m of the seaward boundary of the shelly chenier. The results of line L5 show that the annual transport volume of shells and debris caused by ocean dynamics under normal conditions is equivalent to that under the action of Typhoon In-fa.

6. Conclusions

Based on remote sensing interpretation, field investigation, and GPS-RTK elevation measurement, this paper investigates the beach erosion and progradation process of the shelly chenier in Binzhou, using comparisons between normal and typhoon hydrodynamics. The shelly cheniers in this area can be divided into two types: the first is the tidal channel shelly chenier, which is significantly affected by the tidal current, and the second is the open shelly chenier, which is significantly affected by direct scouring and silting of waves. Influenced by shoreline changes and port construction, the sediment supply is reduced, and the regional marine dynamic action is also weakened [27]; therefore, the wave and current power is insufficient to transport the shells and their debris in the intertidal zone to the shell-beach under normal hydrodynamics. The open shelly chenier is in the process of continuous erosion and regression under the action of normal hydrodynamics, while the tidal channel shelly chenier is gradually progradating due to the action of alongshore current and in–out flow. On the contrary, the continuous action of waves makes the shells and their debris on the open-shell beach finer and transports the shells and their debris to the sea, causing erosion of the shelly chenier. The action of typhoons and other strong winds and waves results in the original accumulation on the open shell–beach being further transported to the land and provides a large amount of shells and debris from the intertidal zone to the shelly chenier. Based on GPS-RTK monitoring data from 2020–2021, it was found that the transport volume of shells and debris caused by a typhoon storm surge is equivalent to the annual transport volume under normal ocean dynamics.

Author Contributions: Conceptualization, M.W., S.Z. and H.W.; Data curation, M.W. and H.W.; Investigation, M.W., H.Z., S.W., P.Y. and H.W.; Project administration, S.Z. and M.W.; Writing—original draft, M.W.; Writing—review & editing, H.Z., S.W., Z.S., S.Z., P.Y. and H.W. All authors have read and agreed to the published version of the manuscript.

Funding: This research was funded by the National Natural Science Foundation of China under contract No. 41806109 and the China Geological Survey Project under contract Nos DD20211301 and DD20189506.

Institutional Review Board Statement: Not applicable.

Informed Consent Statement: Not applicable.

Data Availability Statement: The data used to support the findings of this study are available from the corresponding author upon request.

Acknowledgments: The authors thank Zhihao Zhou, Mengquan Wen, Qinglongliu, and other management workers of Binzhou Shell Dike Islands and Wetlands National Nature Reserve for their help in this investigation. The authors also appreciate the anonymous English editor's constructive comments, which greatly improved both the science and the quality of our original manuscript.

Conflicts of Interest: The authors declare no conflict of interest.

References

1. Russell, E.J.; Howe, H.V. Cheniers of southwestern Louisiana. *Geogr. Rev.* **1935**, *25*, 449–461. [CrossRef]
2. Otvos, E.G.; Price, W.A. Problems of Chenier genesis and terminology: An overview. *Mar. Geol.* **1979**, *31*, 251–263. [CrossRef]
3. Otvos, E.G. Cheniers. In *Encyclopaedia of Coastal Science*; Finkl, C., Makowski, C., Eds.; Springer: Berlin, Germany, 2018; pp. 1–17.
4. Scheffers, A.; Engel, M.; Scheffers, S.; Squire, P.; Kelletat, D. Beach ridge systems-archives for Holocene coastal events? *Prog. Phys. Geogr.* **2012**, *36*, 5–37. [CrossRef]
5. Tamura, T. Beach ridges and prograded beach deposits as palaeoenvironment records. *Earth Sci. Rev.* **2012**, *114*, 279–297. [CrossRef]
6. Nardin, W.; Fagherazzi, S. The role of waves, shelf slope, and sediment characteristics on the development of erosional chenier plains. *Geophys. Res. Lett.* **2018**, *45*, 8435–8444. [CrossRef]
7. Augustinus, P.G.E.F. Cheniers and chenier plains: A general introduction. *Mar. Geol.* **1989**, *90*, 219–229. [CrossRef]
8. Saito, Y.; Wei, H.L.; Zhou, Y.; Nishimura, A.; Sato, Y.; Yokota, S. Delta progradation and chenier formation in the Huanghe (Yellow River) Delta, China. *J. Asian Earth Sci.* **2000**, *18*, 489–497. [CrossRef]
9. Zhao, X.T. Cheniers in Chia: An overview. *Mar. Geol.* **1989**, *90*, 311–320.
10. Wang, Y. The shell coast ridge and the old coastlines of the west coast of the Bohai Bay. *Acta Sci. Natl. Univ. Nankinesis* **1964**, *8*, 424–442.
11. Chen, Y.S.; Li, J.F.; Yang, P.; Wang, F.; Tian, L.Z. AMS 14C ages of marine shells and the residence time effect on the north coastal of Bohai Bay. *North China Geol.* **2021**, *44*, 21–27.
12. Delaune, R.; Jugsujinda, A.; Gambrell, R.; Miao, S. Metal concentrations and trace metal Al and Fe ratios in soil of the Chenier Plain, Southwest Louisiana coastal zone. *J. Environ. Sci. Health A* **2008**, *43*, 300–312. [CrossRef] [PubMed]
13. Draut, A.E.; Kineke, G.C.; Huh, O.K.; Grymes, J.M.; Westphal, K.A.; Moeller, C.C. Coastal mudflat accretion under energetic conditions, Louisiana chenier-plain coast, USA. *Mar. Geol.* **2008**, *214*, 27–47. [CrossRef]
14. Anthony, E.J.; Gardel, A.; Gratiot, N. Fluvial sediment supply, mud banks, cheniers and the morphodynamics of the coast of South America between the Amazon and Orinoco river mouths. *Geol. Soc. Lond. Spec. Publ.* **2014**, *388*, 533–560. [CrossRef]
15. Anthony, E.J.; Gardel, A.; Gratiot, N.; Proisy, C.; Allison, M.A.; Dolique, F.; Fromard, F. The Amazon-influenced muddy coast of South America: A review of mud bank-shoreline interactions. *Earth Sci. Rev.* **2010**, *103*, 99–121. [CrossRef]
16. Shang, Z.W.; Wang, H.; Li, J.F.; Shi, P.X. Land and sea evolution since 11,000 years in the coast of Bohai Bay. *China Min. Mag.* **2018**, *27*, 293–296.
17. Wang, H.; Strydonck, M. Chronology of Holocene cheniers and oyster reefs on the coast of Bohai Bay, China. *Quat. Res.* **1997**, *47*, 192–205. [CrossRef]
18. Wang, H. Palaeoenvironment of the Holocene cheniers and oyster reefs in the Bohai Bay, China. *Quat. Sci.* **1996**, *1*, 71–79.
19. Xu, J.S. Chenier and sea-level change on the coast of Huanghua, Bohai Gulf. *Acta Oceanol. Sin.* **1994**, *16*, 68–77.
20. Zhao, X.T.; Zhang, J.W.; Jiao, W.Q.; Li, G.Y. Chenier ridge on the west coast of Bohai Sea. *Chin. Sci. Bull.* **1980**, *25*, 279–281.
21. Su, S.W. *Palaeoenvironmental Reconstruction of the Holocene Cheniers in the West Coast of Bohai Bay*; Jilin University of China: Jilin, China, 2012; pp. 1–79.
22. Yue, J.; Dong, Y.; Zhang, B.H.; Geng, X.; Liu, X.; Zhao, X.; Mou, L.; Zhang, B.; Han, F. A few of barrier sand bars on the west coast of Bohai bay. *Acta Geol. Sin.* **2012**, *86*, 522–534.
23. Li, S.Y. Preliminary study on relics of coast and culture in the west coast of Bohai Bay. *Acta Archaeol. Sin.* **1962**, *12*, 652–657.

24. Wang, H.; Li, J.F.; Zhang, Y.F.; Li, F. The younger cheniers (shell banks) on the west coast of Bohai Bay: Morphology, structure and polygenetic processes. *Geol. Rev.* **2000**, *46*, 276–287.
25. Xue, C.T. Origin of coastal landforms from the Zhangweixin river mouth to the Tuhai river mouth along the West Coast of the Bohai Sea. *Adv. Mar. Sci.* **2011**, *29*, 330–338.
26. Zhao, Y.L.; Tan, Q.X.; Shi, N.H. Changes of river system in Chinese history, Yellow River. Historical Physical Geography. In *Physical Geography of China*; Science Press: Beijing, China, 1982; pp. 38–86.
27. Working Group on Atlas of Historical Geography, China. *Atlas of Historical Geography*; China Atlas Press: Beijing, China, 1975.
28. Xu, Y.M.; Wang, Y.H. Hydrodynamic response of chenier coast to storm surges on the abandoned Yellow River Delta plain. *Mar. Geol. Quat. Ternary Geol.* **2015**, *35*, 25–32.
29. Zhang, L.K.; Wu, J.Z.; Li, W.R.; Hu, R.J.; Qiu, J.D. Coastline changes and tidal flat evolution in west and south parts of Bohai Bay and affecting factors. *Mar. Geol. Quat. Ternary Geol.* **2014**, *34*, 21–27.
30. Liu, Z.J. *The Sedimentary Characteristics and Evolution of Shell Ridge, North Coast of Shandong Province*; Ocean University of China: Qingdao, China, 2004; Volume 29, pp. 12–17.
31. Du, Y.T.; Huang, H.; Wang, Z.Y.; Liu, Y.X. Evolution of the shell ridge islands on the northern Yellow River Delta. *Mar. Geol. Quat. Geol.* **2009**, *29*, 23–29.
32. Wang, F.; Shang, Z.W.; Li, J.F.; Jiang, X.J.; Wen, M.J.; Shi, P.Q.; Tian, L.Z.; Chen, Y.S.; Yang, P.; Hu, Y.Z.; et al. Research status and protection suggestions of cheniers on Bohai Bay. *Geol. Surv. Res.* **2020**, *43*, 293–316.
33. Wang, F.C.; Yang, P.; Shi, P.X.; Shang, Z.W.; Xiao, G.Q.; Wang, F. Research on the status of Hebei Province's coastline in 2019 based on Landsat OLI images. *North China Geol.* **2021**, *44*, 35–39.
34. Gao, S. Geomorphology and sedimentology of tidal flats. In *Coastal Wetlands: An Ecosystem Integrated Approach*, 2nd ed.; Perillo, G.M.E., Wolanski, E., Cahoon, D., Brinson, M.M., Eds.; Elsevier: Amsterdam, The Netherlands, 2019; pp. 359–381.
35. Wang, Q.; Yuan, G.B.; Zhang, S.; Liu, Z.; Wang, W.; Liu, Z.; Zhuang, Z. Shelly ridge accumulation and sea-land interaction on the west coast of the Bohai Bay. *Quat. Sci.* **2007**, *27*, 775–786.
36. Fu, C.F.; Li, T.; Shi, C.; Gao, Y.; Dong, J.X. Characteristics of the storm surge and UAV disaster investigation caused by the typhoon Lekima (No.1909) in the Bohai Bay. *Mar. Forecast.* **2021**, *38*, 17–23.